J Therm Anal Calorim (2013) 113:395–403
DOI 10.1007/s10973-013-3218-9

Effect of mechanical alloying and annealing on the sintering behaviour of AstaloyCrL powders with SiC and carbon addition

M. Hebda · S. Gądek · M. Skałoń · J. Kazior

Received: 15 November 2012 / Accepted: 23 April 2013 / Published online: 16 May 2013

Abstract Alloying is one of the several effective ways of increasing the properties of iron-based PM materials. Modifying the chemical composition of AstaloyCrL powder by silicon addition offers subsequent, effective way of increasing the properties of iron-based PM materials. However, silicon has a high affinity for oxygen, therefore, its implementation is problematic during the sintering process of mixtured powders. In order to overcome this problem and to obtain a homogeneous composition of low-alloy steel with silicon addition, it seems that mechanical alloying (MA) is the most useful process. In order to better understand the sintering behaviour of low-alloy steel modified by silicon, the aim of the present study was to determine the effect of the MA process on AstaloyCrL powder with the addition of silicon in the form of silicon carbide and 0.4/0.6 mass% graphite on the thermal effects during heating measured by differential scanning calorimeter and thermogravimetry techniques. Removal of lubricants during heating of the blended powders as well as exhaust gases from the furnace were monitored by quadruple mass spectrometry. Furthermore, both a light optical microscope and a scanning electron microscope were used for microstructure analysis. Moreover, Thermo-Calc computer software program were used to calculate the enthalpy changes and the volume fraction of phases.

Keywords Mechanical alloying · AstaloyCrL · Silicon carbide · Mass spectrometry · Pyrolysis · Thermo-Calc

M. Hebda (✉) · S. Gądek · M. Skałoń · J. Kazior
Institute of Material Engineering, Cracow University of Technology, ul. Warszawska 24, 31-155 Kraków, Poland
e-mail: mhebda@pk.edu.pl

Introduction

In recent years, there has been intensive development in powder metallurgy technology. For iron-based PM materials optimal properties could be obtained only when density and chemical composition were considered [1, 2]. Alloying is another effective way of increasing the properties of iron-based PM materials [1]. As an example, AstaloyCrL pre-alloyed powder, produced by Höganäs, with chromium, as a pre-alloying element, along with the presence of carbon improves hardenability of the sintered compacts. Furthermore, chromium is relatively cheap and possesses good recyclability [3, 4]. By silicon addition to the AstaloyCrL alloy powder, suitable choice of sintering parameters and heat treatment, it is possible to modify the microstructure of the sintered material (e.g. possible to obtain bainitic–austenitic microstructure). Due to the excellent combination of toughness and strength, bainitic–austenitic dual phase steels with silicon addition have many applications as structural components in the industry. However, silicon has a high affinity for oxygen, therefore, its implementation is problematic during the sintering process of mixtured powders. In order to obtain a homogeneous composition of low-alloy steel with silicon addition, it seems that mechanical alloying (MA) is the most useful process [5]. The MA process has been widely used to produce alloys and compounds that are difficult or even impossible to obtain via conventional melting and casting techniques [6, 7]. The other problem is the influence of lubricants on the milling as well as on the sintering process. The PM company usually introduces a different kind of lubricant into the powder mixture. Lubricants are typically added, from 0.5 to 1.5 mass%, to the metal powder to aid compaction uniformity and to decrease die-wall friction during compaction and ejection, thereby reducing die wear. Lubricants can also act as temporary binders to enhance the

Table 1 Notation, chemical composition of the powder mixtures and kind of applied treatment of the investigated powders mixture

Notation	Chemical compositions	Treatment
1	AstaloyCrL + 3 mass% SiC + 0.6 mass% C	Mixed powder (without stearic acid, not MA)
2	AstaloyCrL + 3 mass% SiC + 0.4 mass% C	Directly after MA process
3	AstaloyCrL + 3 mass% SiC + 0.6 mass% C	Directly after MA process
4	AstaloyCrL + 3 mass% SiC + 0.4 mass% C	After MA process 1 h annealing at 600 °C in H_2 atmosphere
5	AstaloyCrL + 3 mass% SiC + 0.6 mass% C	After MA process 1 h annealing at 600 °C in H_2 atmosphere

'green' strength of a metal part. In the MA process, lubricants can also act as a process control agent (PCA) with the aim of controlling the MA process and, in principle, to avoid powder particle agglomeration due to excessive cold welding [8–12]. The remaining lubricant within the compact may restrict densification during sintering, can have a negative impact on the part's surface and appearance, and they can dramatically lower the part's mechanical properties. Therefore, it must be removed in the early stages of heating [13, 14]. This issue has become essential in the production of powder metallurgy parts [10, 11, 14].

The aim of this paper was to study the influence of the mechanical alloying process of AstaloyCrL with 3 mass% of SiC and carbon addition on thermal effects measured during sintering by differential scanning calorimeter (DSC) and thermogravimetry (TG) techniques. For analysis of the removal of lubricants during sintering of the blended powders, the exhaust gases from the furnace were monitored online by quadruple mass spectrometry (QMS). Furthermore, a light optical microscope and a scanning electron microscope were used for microstructure analysis. Moreover, Thermo-Calc computer software program was used to calculate the enthalpy changes and the volume fraction of phases.

Experimental

Specimens for thermal analysis and the following sintering process were prepared by the mechanical alloying of AstaloyCrL powders (water-atomised iron powder with addition of 1.5 mass% Cr and 0.2 mass% Mo manufactured and supplied by Höganäs) with 3 mass% silicon carbide (supplied by Sigma-Aldrich) and 1 mass% stearic acid (supplied by Sigma-Aldrich). Stearic acid ($CH_3(CH_2)_{16}COOH$) was added only to the powder mixture as the agent with the aim of controlling the mechanical alloying process and, in principle, to avoid powder particle agglomeration. For MA, a highly energetic planetary mono ball mill (Fritsch, Pulverissette 6 model) was used. The process was carried out in a tempered steel container (500 mL volume) equipped with grinding balls Ø 10 mm (ball bearing steel AISI 52100) in a

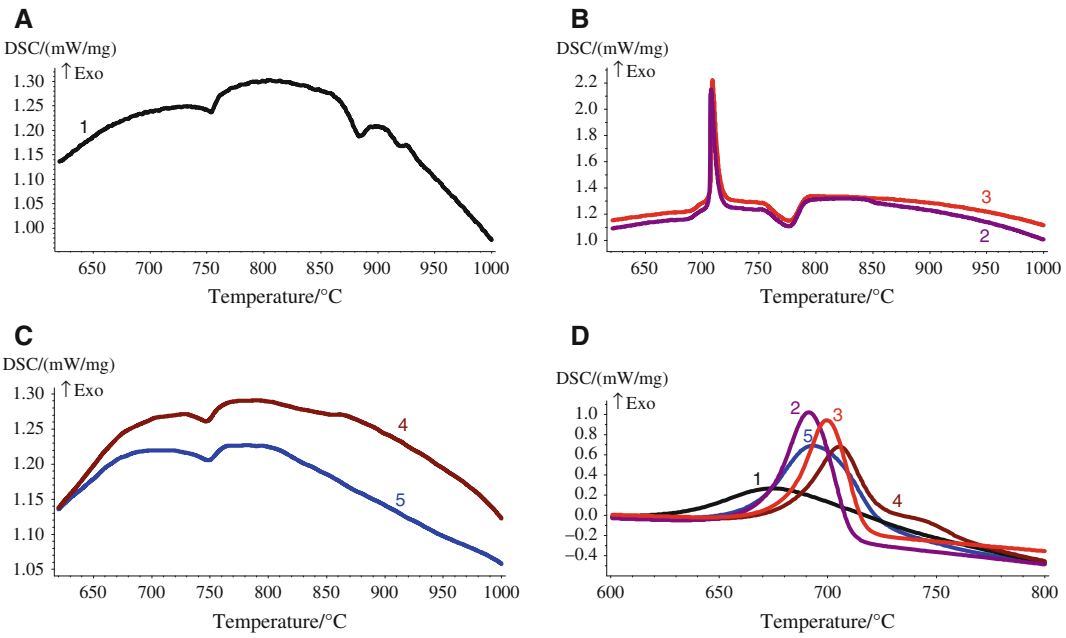

Fig. 1 DSC curves of the AstaloyCrL powder with the addition of 3 mass% SiC, 1 mass% stearic acid and 0.4 or 0.6 C mass% recorded upon heating of the samples: **a** mixed powder, **b** directly after MA process, **c** after annealing at 600 °C in H_2 atmosphere and **d** all specimens recorded during cooling. Notation according to Table 1

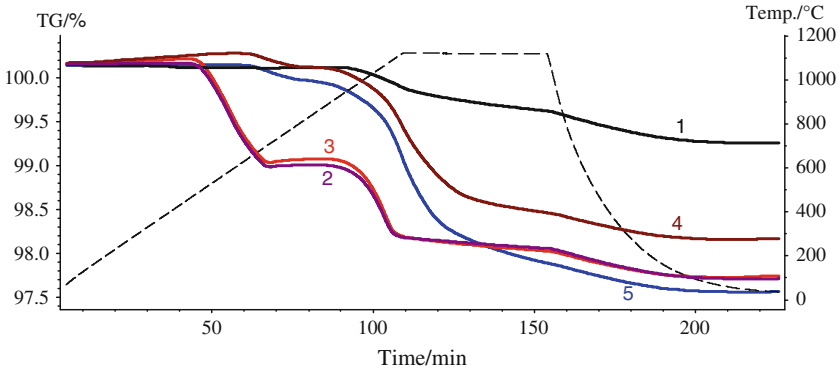

Fig. 2 TG curves of the investigated powder compositions recorded during whole temperature treatment (*dotted line* presents the temperature profile). Notation according to Table 1

Table 2 Evolution of mass changes with temperature ranges of analysed compositions

Notation	1 step			2 steps			3 steps			4 steps		
	Onset/ °C	Endset/ °C	Mass changes/%	Onset/ °C	Endset/ °C	Mass changes/%	Onset/ °C	Endset/ °C	Mass changes/%	Onset/ °C	Endset/ °C	Mass changes/%
1	914	1,121	−0.26	1,121	1,081	−0.24	1,081	45	−0.36	–	–	–
2	470	723	−1.18	911	1,105	−0.79	1,105	1,052	−0.15	1,052	40	−0.34
3	470	723	−1.17	911	1,105	−0.85	1,105	1,052	−0.20	1,052	40	−0.29
4	630	814	−0.15	893	1,120	−1.45	1,120	40	−0.48	–	–	–
5	620	804	−0.17	804	1,120	−1.64	1,120	40	−0.77	–	–	–

vacuum atmosphere (10^{-3} mbar). The ratio of powder mass to ball mass was at a level of 1:10. The milling time was 6 min, intermission period 30 min, number of cycles 100, and rotary speed 500 rev min^{-1}. Due to the high hardening of powders after the MA process the prepared mixture was divided for two parts. Carbon (with the addition of 0.4 or 0.6 mass%) was added to one part directly after the MA process. The second portion was annealed for 1 h at 600 °C in hydrogen atmosphere to reduce the intensity of stress and to decrease powder hardness for the future possibility of die compaction. After the annealing, carbon was added in the amount of 0.4 or 0.6 mass% to the powders mixture. The powders mixtures with carbon addition were mixed using Turbula equipment for 24 h. Thermal measurements were performed with STA 409 CD (Netzsch) advanced coupling techniques (DSC/TG), including evolved gas analysis by quadruple mass spectrometry (QMS 403/5 SKIMMER). Each thermal measurements were repeated two times. The DSC experiments were carried out using a closed alumina crucible (85 μL; there was a 50 μm hole in the lead), with about 151 mg of loose powder samples under a dynamic argon (5.0) atmosphere (flow rate 80 mL min^{-1}). The heating rate to the isothermal step at 1,120 °C was 10 °C min^{-1}. The isothermal step lasted 45 min. The cooling rate from the isothermal step to room temperature was 60 °C min^{-1}. An empty, closed alumina crucible was used as a reference. Temperature and sensitivity (by the melting heat) of apparatus was calibrated using indium, tin, bismuth, zinc, aluminium, silver and gold as a standard. The on-line gas analysis was studied by QMS with an electron ionisation source. The spectrometer was operated in multiple ion detection (MID) mode. The QMS was checked using calcium oxalate monohydrate (Fluka). The DSC/TG/QMS data were analysed using Proteus software (ver. 5.2.0) from Netzsch. The metallographic investigation was conducted using a light optical microscope (model Nexus) on specimens etched: (i) Alkaline sodium picrate: 100 mL water, 2 g picric acid, 25 g NaOH; use 90–100 °C, (ii) Murakami's: 100 mL water, 10 g NaOH, 10 g K3 $Fe(CN)_6$; mix fresh, use at 20 °C, (iii) Groesbeck's: 100 mL water, 4 g NaOH, 4 g $KMnO_4$; use at 20 °C, (iv) 10 % ammonium persulfate: 100 mL water, 10 g $(NH_4)_2S_2O_8$, at 6 V DC, 10 s [15]. Furthermore, the chemical composition of the specimens was checked using a scanning electron microscope (SEM), Jeol JSM-5510LV, with an energy dispersive spectrometer (EDS), IXRF Systems Model 500 Digital Processing. The etched samples were examined using backscattered electrons. The generated radiations of Fe, Cr, Mo and Si X-ray lines were measured. Thermo-Calc software v.5 with a TCFE6 database was used to calculate the mole fraction of phases and the enthalpy changes (a simulation of the utilised global minimisation of Gibbs free energy). The following phases were considered in the simulation: liquid, ferrite, austenite, $M_{23}C_6$, SiC (due to the expected phase composition, where M—Metal). Pressure applied: 101,325 Pa. Table 1 shows the notation, chemical

composition of the powder mixtures and kind of applied treatment of the investigated powders mixture.

Results and discussion

Figure 1a presents the results of DSC measurements of only the mixed powder (without the MA process and stearic acid). The recorded curve showed two small endothermic peaks. The position of the first peak (T_{peak} 754 °C) corresponds to the Curie temperature, while the second peak (T_{peak} 884 °C) can be ascribed to the $\alpha \rightarrow \gamma$ transformation. The DSC traces for the powders analysed directly after the mechanical alloying process are presented in Fig. 1b and show significant changes in the recorded traces as compared to the mixed powder without the MA process. The relatively large exothermic peaks occurring between 687 and 726 °C were detected only for samples investigated directly after the MA process. The amount of carbon addition had no influence on this effect.

DSC measurements proved that the exothermal heat release is irreversible. After the annealing process (the as-milled specimens) up to 600 °C, in a following DSC measurement the broad exothermal heat release disappeared (Fig. 1c) as compared to samples investigated after MA process (Fig. 1b). Only small endothermic peaks were detected. Therefore, the exothermal effect is supposed to be related to a structural relaxation and chemical ordering as well as stress relaxation of the as-milled metastable phases and crystallisation.

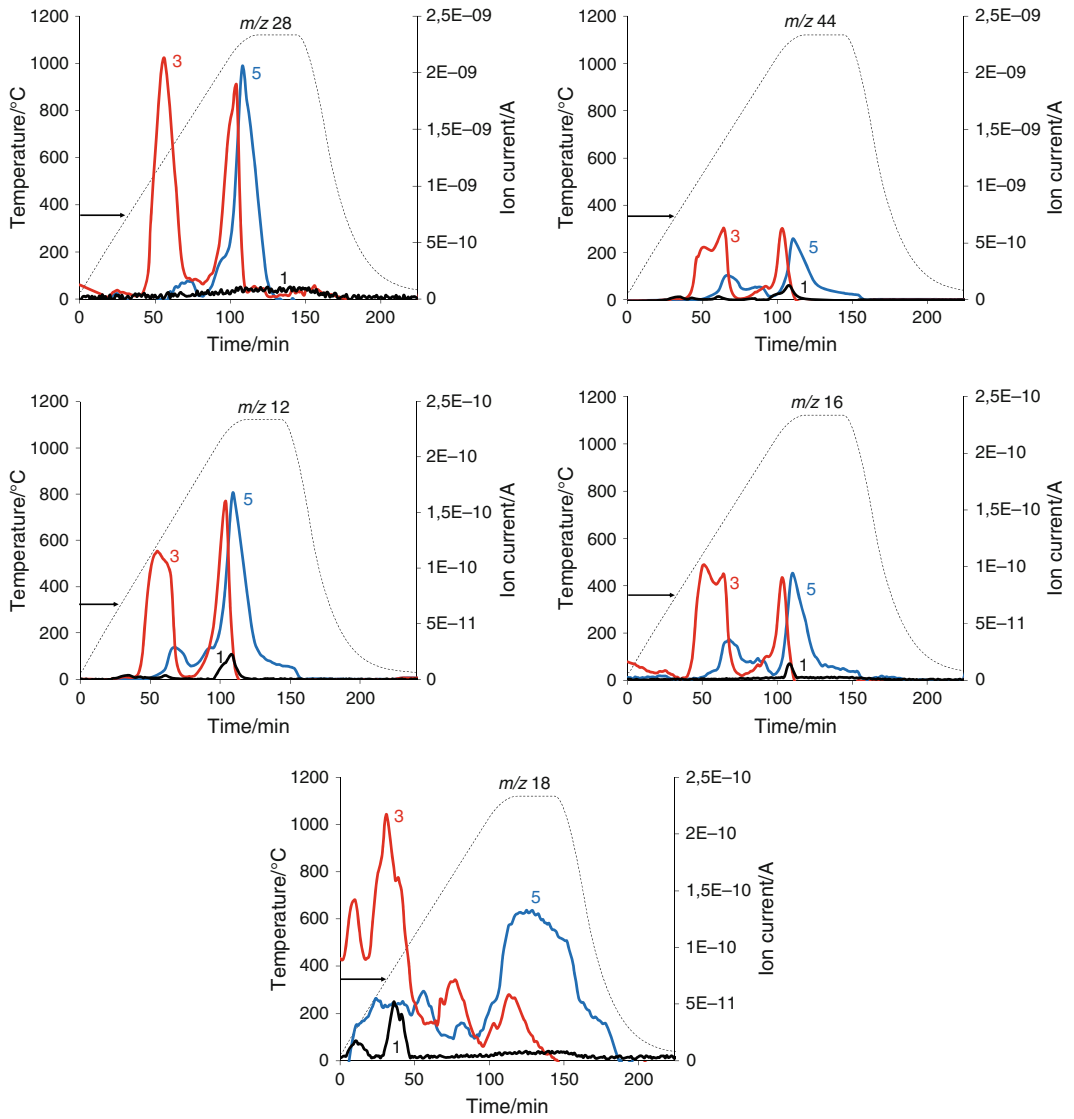

Fig. 3 Mass spectrum obtained via MID mode as well as the process temperature as a function of process time for the: *1* base powder, *3* powder directly after the MA process, *5* powder after the annealing process (*dotted line* presents the temperature profile, notation according to Table 1)

Table 3 Relative ion currents for CO and CO_2 products

	m/*z*	Relative intensity/%
Carbon monoxide (CO)	28	100
	12	4.5
	29	1.1
	16	0.9
Carbon dioxide (CO_2)	44	100
	28	11.4
	16	8.5
	12	6

Similar exothermal phenomena in the investigation of the solid-state reaction in the nanocrystalline Fe/SiC composites prepared by mechanical alloying were also registered by Koch et al. [16] as well as for the another investigated alloyed system produced by mechanical alloying [17–20].

Furthermore, during heating (above 730 °C) for the powders analysed directly after the mechanical alloying process (Fig. 1b) as well as for the powders investigated after the annealing process (Fig. 1c), a strong endothermic peak was observed, which can be explained as the result of an overlapping of the magnetic transition at the Curie temperature and the $\alpha \rightarrow \gamma$ transformation. This effect is correlated by the MA process and has been described in another work [10].

During cooling, one exothermic peak was registered (with the position of maximum peaks at about 690 °C) for all of the investigated samples. However, during cooling samples of powders directly after the MA process showed the highest intensity of the exothermic effect in a narrow range of temperatures, as compared to the exothermic effect for the powder mixture without the MA process, which occurred in a broad range of temperatures (Fig. 1d).

Figure 2 presents the results of the TG measurements of the investigated powder compositions recorded during whole temperature treatment. It is clear that the MA process had a strong influence on the changes in the TG curves (in comparison to the powder mixture without MA). This phenomenon was probably correlated with the fragmentation of particles, accumulated energy during MA and the presence of lubricant additions (which can also be disintegrated in the course of the MA process [10]). Only for the powders analysed directly after MA, four steps of mass loss were registered. However, the first two steps are the most intensive. The first decrease of mass was the result of the lubricant evaporation process (and had the most intensive character) which occurred between 470 and 723 °C. The second step, probably associated with a reduction of oxides, was also recorded before the isothermal temperature (which started at around 900 °C). During the sintering process only a slight loss of mass was detected. On the other hand, the annealing process also intensely affected the TG curves of the investigated mixtures. The first step of mass loss (in a temperature range between around 500 and 800 °C) was reduced (as a result of the burning of lubricants during annealing of the powder), but the highest thermogravimetry mass changes were observed during the isothermal step. For powder without MA on the TG curve a small loss of mass was recorded after exceeding a temperature of 940 °C. In Table 2 the evolution of mass changes with temperature for all of the investigated compositions was presented.

The mass spectrometer allowed to interpret the recorded TG traces. From the mass spectrometry curves presented in Fig. 3, it was observed that the main products of the evaporated gases (independently of the chemical composition) were carbon monoxide and carbon dioxide (with an intensity of 10E-9). The most intense masses for CO and CO_2 according to the NIST library were presented in Table 3.

In general, powders analysed directly after the MA process had two comparable maxima of emitted gases observed as peaks at 595 and 1,066 °C. The first effect is

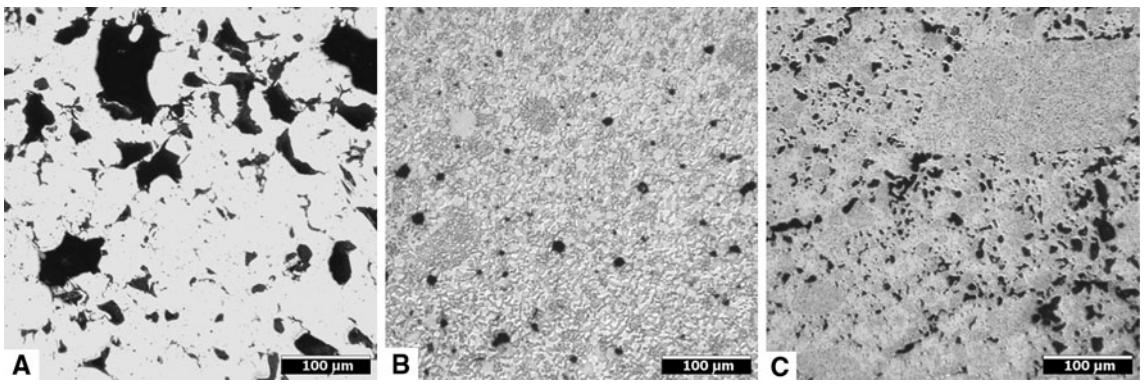

Fig. 4 Microstructures of sintered AstaloyCrL with 3 mass% SiC and 0.6 mass% C **a** mixed powder (not MA) **b** directly after MA process **c** after 1 h annealing at 600 °C in H_2 atmosphere, non-etched

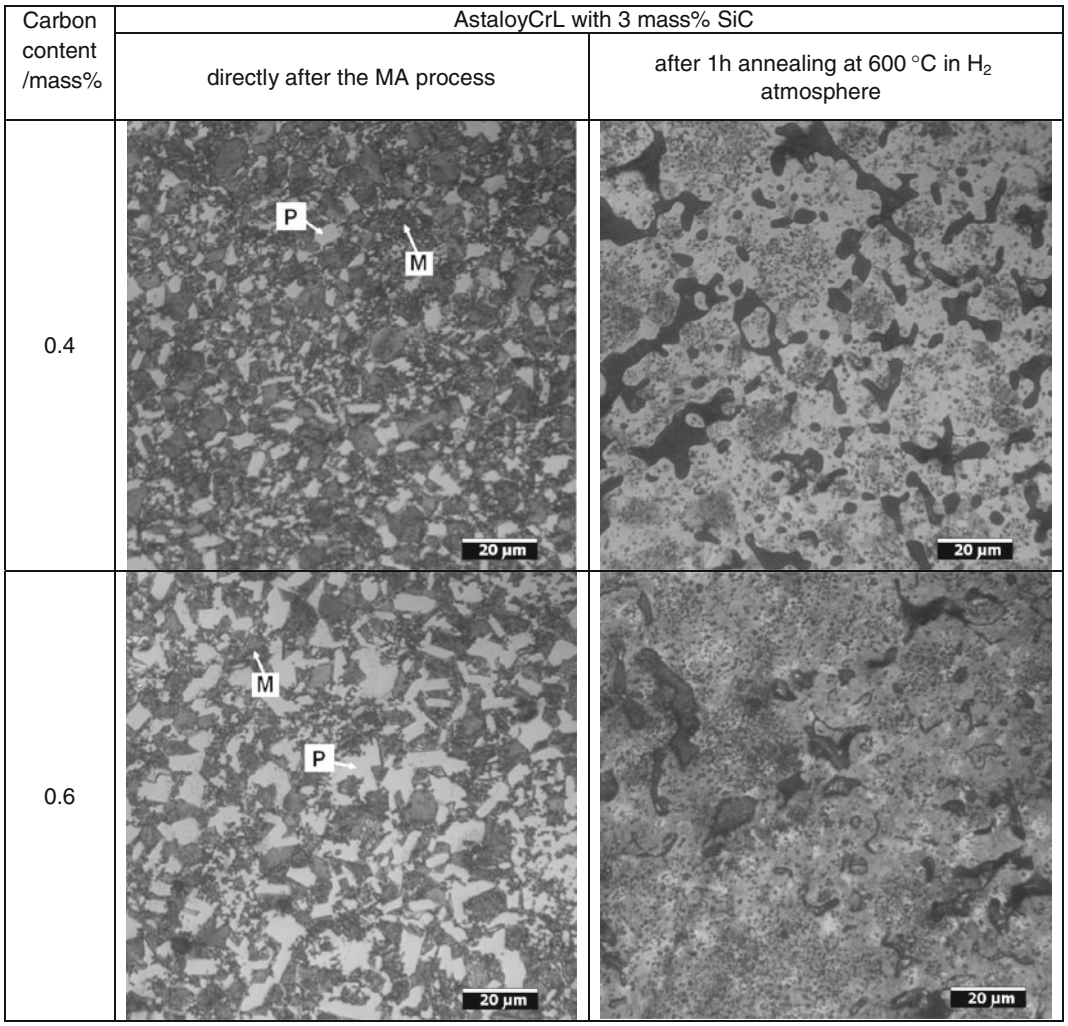

Fig. 5 Microstructures of sintered AstaloyCrL with the addition of 3 mass% SiC and 0.4 mass% C or 0.6 mass% C (in order of microstructures) directly after the MA process (*left*) or after 1 h annealing at 600 °C in H_2 atmosphere (*right*) etched, *M* matrix, *P* precipitation

Table 4 Chemical composition of sintered AstaloyCrL with the addition of 3 mass% SiC and 0.6 mass% C investigated by SEM with a microprobe

Type of area	Elements/mass%			
	Fe	Cr	Mo	Si
Matrix/dark area	95.66 ± 2.58	1.12 ± 0.04	0.49 ± 0.21	2.73 ± 0.07
Precipitation/bright area	95.71 ± 0.41	3.57 ± 0.27	0.48 ± 0.07	0.24 ± 0.12

Table 5 The microhardness HV0.01 of sintered AstaloyCrL with the addition of 3 mass% SiC and 0.4 or 0.6 mass% C directly after MA process or after 1 h annealing at 600 °C in H_2 atmosphere

Carbon content/mass%	AstaloyCrL with 3 mass% SiC			
	Directly after MA process		After 1 h annealing at 600 °C in H_2 atmosphere	
	Matrix	Precipitation	Matrix	Precipitation
0.4	341 ± 37	1108 ± 128	324 ± 13	–
0.6	410 ± 42	1279 ± 203	355 ± 43	–

associated with the process of the removal of lubricants, which may intensify the sintering process by a strong increase in hydrocarbon, hydrogen and carbon products as a result of the disintegration of the chemical chain of stearic acid by the MA process [10, 13].

Moreover, the first CO-peak, indicating interaction of the plain graphite with the surface iron oxides (first step of carbothermal reduction). This effect is especially evident for the investigated powder directly after the mechanical alloying process.

On the basis of the obtained results (the CO, C, CO_2 peaks), it could be concluded that in high temperatures (above 1,000 °C), the dominant mechanism for the reduction of oxides (more stable surface oxides) and the activation of the sintering process was the carbothermal reaction [21–23].

Both mechanisms are observed for the tested powders after the mechanical alloying process; however, they are various in the intensity of their occurrence. Samples of powder after annealing emitted a maximum of the product at 1,120 °C (the beginning of the isothermal step) and only for some of the investigated mass ions was a small effect at 700 °C also detected. During isothermal sintering, more intense hydrogen and water (*m*/*z* 18) products were registered, which explains the rapid mass loss observed in the TG curves. Moreover, signals from the hydrocarbon products (e.g. *m*/*z* 16, *m*/*z* 29, *m*/*z* 44) were also detected.

Powders after mechanical alloying process were characterized by a much smaller particles, higher accumulated energy and deformation, regions of exposed pure metallic surface which caused the higher mass loss on TG curves (Fig. 2) as well as increased carbothermal reduction (Fig. 3) than for powder mixture without MA.

Figure 4 shows the microstructures of the investigated AstaloyCrL sintered powder with 3 mass% SiC and 0.6 mass% C (after DSC measurements of loose powders) before etching.

As can be seen in Fig. 4a, porosity of mixed powder (without MA process) is locally large and interconnected (typical for the intermediate stage of sintering). The microstructure of the samples after the mechanical alloying process looks different and is characterised by small, spherical, separated precipitates evenly distributed over the entire volume of the material. Moreover, an additional phase is visible even without etching (Fig. 4b). After the annealing treatment and the following sintering process, a greater share of volume porosity was detected (as shown in Fig. 4c). In principle, the morphology of the porosity is rather complex, with isolated spherical shapes and fine, interconnected pores.

Only samples sintered directly after the mechanical alloying process after etching revealed precipitates. In Fig. 5, they are shown as polyhedral, bright, large precipitates. Their quantity increased with an increasing carbon content introduced additionally.

Microstructures of mixed powder (not MA) and after 1 h annealing at 600 °C in H_2 atmosphere looked similarly. For this reason, in Fig. 5, microstructures obtained directly after the MA process was compared with the annealed. Furthermore, bainite structure was not received because the heat treatment was not applied (e.g. sinter-austempering) and the sample cooling rate was too small.

In order to identify the type of observed precipitates, the chemical composition of the matrix and precipitates using scanning microanalysis was investigated. The results are presented in Table 4. It was found that the areas of the precipitates are much richer in chrome. The obtained results suggest the formation of $M_{23}C_6$ type carbides. Moreover, microhardness HV0.01 of observed precipitates were about 3 times higher than matrix (Table 5).

Furthermore, the formation of $M_{23}C_6$ type carbides was confirmed by selective etching [15]. Four different reagents were used. Carbides observed in the microstructure identical react as $M_{23}C_6$ after etched described in [15].

The results of the DSC measurement for AstaloyCrL with 3 mass% SiC and 0.6 mass% C obtained during cooling were verified by Thermo-Calc software. A good relationship was found between the experimental enthalpy changes determined by DSC measurement (Fig. 1d, with value of ~ 59 J g^{-1} independent of type of investigated powder compositions) and the calculated enthalpy changes from the Thermo-Calc software (Fig. 6, which confirms the presence of exothermal effect) as well as the calculated heat capacity changes with a value 50 J g^{-1} from the Thermo-Calc software (Fig. 7).

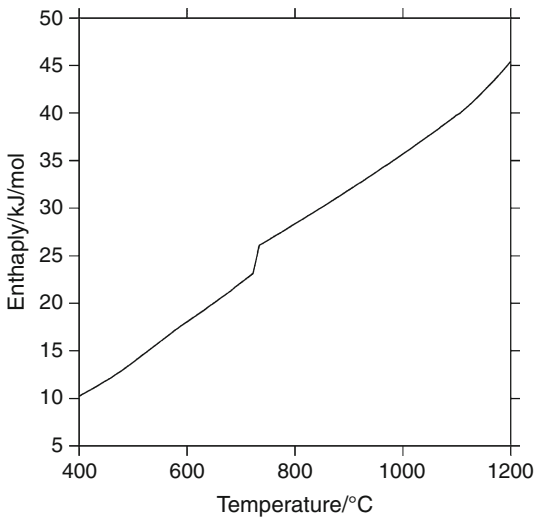

Fig. 6 Enthalpy changes versus temperature for AstaloyCrL with 3 mass% SiC and 0.6 mass% C (from Thermo-Calc)

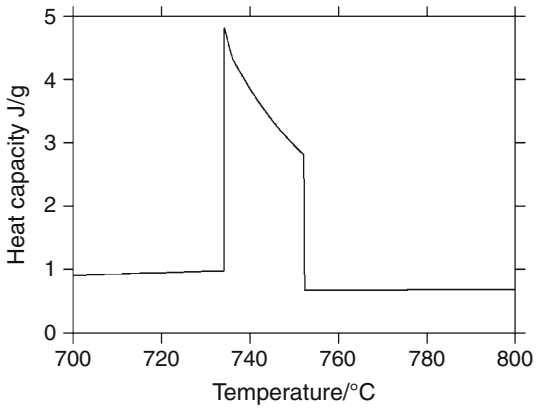

Fig. 7 Heat capacity changes versus temperature for AstaloyCrL with 3 mass% SiC and 0.6 mass% C (from Thermo-Calc)

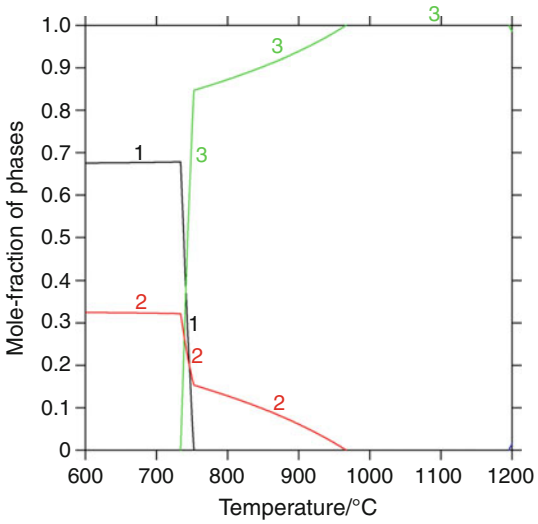

Fig. 8 Mole fraction of phases (*1* ferrite, *2* $M_{23}C_6$, *3* austenite) versus temperature for AstaloyCrL with 3 mass% SiC and 0.6 mass% C (from Thermo-Calc)

Moreover, from an analysis of the diagram designed by the Thermo-Calc software, it can be assumed that the $M_{23}C_6$ carbide may precipitate during cooling of the investigated powder (Fig. 8). This effect occurs at temperatures which correspond to the transformation of austenite into ferrite. Furthermore, from comparison the data from Thermo-Calc with the observation of microstructures, it is evident that precipitation of the $M_{23}C_6$ carbides well corresponds to the microstructures presented in Fig. 5. for samples sintered directly after the mechanical alloying process. Concluding, the accumulated energy during the MA process, no equilibrium state of the sintered powders directly after MA and thereby, the occurring intensification of the sintering process in the material had a crucial impact on the obtained structure and precipitation of the carbides. For annealed samples, the activation energy is lower as compared with samples after MA and in consequences after sintering process their microstructure is similar to the microstructure of mixed powder without MA process (carbides precipitates were not observed).

Conclusions

It was found that the mechanical alloying process had a strong influence on the sintering behaviour of the investigated powder mixture, AstaloyCrL, with the addition of 3 mass% SiC and 0.4 or 0.6 mass% C. After the MA process, the powder mixture analysed by DSC exhibited a strong exothermal effect during heating and a strong endothermic peak as a result of overlapping of the magnetic transition (at the Curie temperature) and the $\alpha \rightarrow \gamma$ transformation. Furthermore, for samples investigated directly after the MA process, the earliest mass loss (at *c.*470 °C) and the highest decreases of mass took place before the isothermal step of the sintering process. Also, four-step decompositions on the TG traces were observed. On the other hand, after the annealing process, the powder showed only a slight effect from the magnetic transition. The TG curves illustrated the highest mass loss during the isothermal step (on the temperature profile). QMS measurements of gaseous products allowed us to interpret the recorded TG traces. The main products of the evaporated gases (independently of the chemical composition) were carbon monoxide, carbon dioxide, and hydrocarbon products. The amount of carbon addition had no important influence of observed effects. It was also found that the MA process significantly influences the type of obtained microstructure and enhanced precipitation of carbides.

Acknowledgments Authors would like to thank the Polish Ministry of Science and Higher Education for support of this work with Grant No NN508 393237.

References

1. Xiao ZY, Ke MY, Fang L, Shao M, Li YY. Die wall lubricated warm compacting and sintering behaviors of pre-mixed Fe–Ni–Cu–Mo–C powders. J Mater Process Technol. 2009;209:4527–30.
2. Engstrom U, Milligan D, Klekovkin A. Mechanical properties of high performance chromium materials. Adv Powder Metall Part Mater. 2006;7:21.
3. Johansson M. Expanding opportunities with chromium. Met Powder Rep. 1999;54:22.
4. Danninger H, Kremel S, Molinari A, Marcu Puscas T, Torralba JM, Campos M, Yo Y. In: Proceedings of PM 2011 Congress and Exhibition on Powder Metallurgy, Nice, France, October 22–24. 2001. p. 28–33.

5. Azadbeh M, Ahmadi NP. Effect of alloying contents and processing factors on the microstructure and homogenization of Si alloyed Cr–Mo sintered steels. Curr Appl Phys. 2009;9:777–82.
6. El-Eskandarany MS. Mechanical alloying for fabrication of advanced engineering materials. Norwich: Wiliam Andrew Publishing; 2001.
7. Suryanarayana C, Ivanov E, Boldyrev VV. The science and technology of mechanical alloying. Mater Sci Eng A. 2001;304–306:151–8.
8. Shaw L, Luo H, Villegas J, Miracle D. Compressive behavior of an extruded nanocrystalline Al–Fe–Cr–Ti alloy. Scripta Mater. 2004;50:921–5.
9. Neamtu BV, Isnard O, Chicinas I, Vagner C, Jumate N, Plaindoux P. Influence of benzene on the Ni3Fe nanocrystalline compound formation by wet mechanical alloying: an investigation combining DSC, X-ray diffraction, mass and IR spectrometries. Mater Chem Phys. 2011;125:364–9.
10. Hebda M, Gądek SZ, Kazior J. Thermal characteristics and analysis of pyrolysis effects during the mechanical alloying process of Astaloy CrM powders. J Therm Anal Calorim. 2012;108(2):453–60.
11. Hebda M, Gądek SZ, Kazior J. Influence of the mechanical alloying process on the sintering behaviour of Astaloy CrM powder mixture with silicon carbide addition. Arch Metall Mater. 2012;57(3):733–43.
12. Pieczonka T, Kazior J, Szewczyk-Nykiel A, Hebda M, Nykiel M. The effect of the atmosphere on sintering of Alumix 431D powder. Powder Metall. 2012;55(5):354–60.
13. Hebda M, Laska M, Szechyńska-Hebda M. Application of a device used for observation of controlled thermal processes in a furnace: examples of delubrication, oxidation, melting, pyrolysis and combustion. J Therm Anal Calorim. doi:10.1007/s10973-013-3157-5.
14. Baum MM, Becker RM, Lappas AM, Moss JA, Apelian D, Saha D, Kapinus VA. Lubricant pyrolysis during sintering of powder metallurgy compacts. Metall Mater Trans B. 2004;35B:381–92.
15. Voort GV, Manilova E, Michael JR, Lucas GM. A study of selective etching of carbides in steel. Microsc Microanal. 2004;10(02):76–7.
16. Koch CC, Shen TD, Wang KY, Quan MX, Wang JT. Solid-state reaction in nanocrystalline Fe/SiC composites prepared by mechanical alloying. J Mater Sci. 1997;32:3835–9.
17. Guan ZQ, Pfullmann Th, Oehring M, Bormann R. Phase formation during ball milling and subsequent thermal decomposition of Ti–Al–Si powder blends. J Alloy Compd. 1997;252:245–51.
18. Gaffet E, Harmelin M. Crystal-amorphous phase transition induced by ball-milling in silicon. J Less Common Met. 1990;157(2):201–22.
19. Fadeeva VI, Leonov AV. Amorphization and crystallization of Al–Fe alloys by mechanical alloying. Mater Sci Eng A. 1996; 206:90–4.
20. Bolarin-Miró AM, Sánchez-De Jesús F, Torres-Villaseñor T, Cortés-Escobedo CA, Betancourt-Cantera JA, Betancourt-Reyes JI. Amorphization of Co-base alloy by mechanical alloying. J Non Cryst Solids. 2011;357:1705–9.
21. Danninger H, Gierl C. New alloying systems for ferrous powder metallurgy precision parts. Sci Sinter. 2008;40:33–46.
22. Danninger H, Gierl C. Processes in PM steel compacts during the initial stages of sintering. Mater Chem Phys. 2001;67:49–55.
23. Hryha E, Gierl C, Nyborg L, Danninger H, Dudrova E. Surface composition of the steel powders pre-alloyed with manganese. Appl Surf Sci. 2010;256:3946–61.